Parasites & Vectors

RESEARCH Open Access

Contribution of parasite and host genotype to immunopathology of schistosome infections

Kathrin S. Jutzeler[1,2*], Winka Le Clec'h[1], Frédéric D. Chevalier[1] and Timothy J. C. Anderson[3*]

Abstract

Background The role of pathogen genotype in determining disease severity and immunopathology has been studied intensively in microbial pathogens including bacteria, fungi, protozoa and viruses but is poorly understood in parasitic helminths. The medically important blood fluke *Schistosoma mansoni* is an excellent model system to study the impact of helminth genetic variation on immunopathology. Our laboratory has demonstrated that laboratory schistosome populations differ in sporocyst growth and cercarial production in the intermediate snail host and worm establishment and fecundity in the vertebrate host. Here, we (i) investigate the hypothesis that schistosome genotype plays a significant role in immunopathology and related parasite life history traits in the vertebrate mouse host and (ii) quantify the relative impact of parasite and host genetics on infection outcomes.

Methods We infected BALB/c and C57BL/6 mice with four different laboratory schistosome populations from Africa and the Americas. We quantified disease progression in the vertebrate host by measuring body weight and complete blood count (CBC) with differential over a 12-week infection period. On sacrifice, we assessed parasitological (egg and worm counts, fecundity), immunopathological (organ measurements and histopathology) and immunological (CBC with differential and cytokine profiles) characteristics to determine the impact of parasite and host genetics.

Results We found significant variation between parasite populations in worm numbers, fecundity, liver and intestine egg counts, liver and spleen weight, and fibrotic area but not in granuloma size. Variation in organ weight was explained by egg burden and intrinsic parasite factors independent of egg burden. We found significant variation between infected mouse lines in cytokine levels (IFN-γ, TNF-α), eosinophils, lymphocytes and monocyte counts.

Conclusions This study showed that both parasite and host genotype impact the outcome of infection. While host genotype explains most of the variation in immunological traits, parasite genotype explains most of the variation in parasitological traits, and both host and parasite genotypes impact immunopathology outcomes.

Keywords Host-parasite interaction, Immunopathogenesis, *Schistosoma mansoni*, BALB/c mouse, C57BL/6 mouse

Background

Pathogen genetic variation can play a crucial role in shaping immunopathology within the host. The recent COVID-19 pandemic serves as a pertinent example as the emergence of new variants of SARS-CoV-2 led to changes in pathogenicity, immunity and symptomatology in infected individuals [1–3]. Similar observations have been made in the fields of bacteriology and parasitology. *Escherichia coli* genotypes exhibit a spectrum of disease severity ranging from asymptomatic to severe [4, 5], and parasite genotype explains 83% of the variation in

*Correspondence:
Kathrin S. Jutzeler
kjutzeler@txbiomed.org
Timothy J. C. Anderson
tanderso@txbiomed.org
[1] Host Parasite Interaction Program, Texas Biomedical Research Institute, P.O. Box 760549, San Antonio, TX 78245, USA
[2] UT Health, Microbiology, Immunology & Molecular Genetics, San Antonio, TX 78229, USA
[3] Disease Intervention and Prevention Program, Texas Biomedical Research Institute, P.O. Box 760549, San Antonio, TX 78245, USA

mortality from visceral leishmaniasis [6]. Yet, we know little about the impact of helminth genetic variation on disease severity. Helminths infect approximately 25% of the world's human population and are ubiquitous parasites of vertebrates, invertebrates and plants [7, 8]. In specific cases, such as *Schistocephalus solidus* tapeworms of sticklebacks, host immune gene expression and immunological parameters vary depending on the parasite population they are infected with [9]. Moreover, genetic variation impacts infection rate, egg burden per cyst and egg hatching rate in the sugarbeet nematode *Heterodera schachtii*, with implications for pathogenicity in plants [10]. Different *Trichinella spiralis* nematode isolates exhibit significant variation in infection clearance, larval burden and host-inflammatory response in mammalian hosts [11, 12]. These examples suggest that parasite genetic variation may have a profound impact on host responses and pathogenicity in helminth infections across diverse species.

Schistosoma mansoni, a blood fluke prevalent in Africa, the Caribbean and South America, causes significant morbidity and mortality in infected people because of a vigorous immune response to schistosome eggs and granuloma formation around eggs that become lodged in ectopic tissues, causing inflammation, fibrosis and portal hypertension [13]. This parasite provides a tractable model organism for investigating the influence of helminth genetic variation on immunopathology, because it can be maintained in the laboratory using rodents as definitive hosts and aquatic snails as intermediate hosts. Schistosomes vary in multiple heritable traits including drug resistance and snail host specificity [14–17]. We have previously demonstrated dramatic differences in cercarial shedding numbers and mortality of intermediate snail hosts infected with two different parasite populations from Brazil, SmBRE or SmLE [18]. Low or high shedding populations derived from crosses between these two parasite populations also varied in life history traits in the rodent host. Low shedding parasites showed lower fecundity, reduced hepatosplenomegaly and hepatic fibrosis in mice than high shedding parasites [19].

The striking differences between these two populations led us to hypothesize that parasite genotype may influence other life history traits and immunopathology in the vertebrate mouse host. Several studies support this notion: Anderson and Cheever [20] first documented significant differences in worm and egg burden when mice were infected with *S. mansoni* field isolates obtained from different geographical regions. Subsequent studies utilizing laboratory-maintained schistosome populations have further examined various parameters including egg dimensions and granuloma burden/area in the liver and intestine (Table 1) [21–23].

We maintain four distinct *S. mansoni* populations in our laboratory (SmEG from Egypt, SmLE and SmBRE from Brazil and SmOR, descended from the SmHR population [24] from Puerto Rico), which we used in this study. These parasite populations show distinctive phenotypes: SmLE shows eightfold higher cercarial production than SmBRE as well as larger sporocysts, higher infectivity to mice and higher fecundity [18, 19]; SmOR is an oxamniquine resistant population homozygous for the deletion in amino acid 142 in *SmSULT-OR* [25]; SmEG is the only population with African origin. Our central aim was to investigate the impact of parasite genetics on immunopathology while accounting for host genetic differences. To do this, we infected mice with schistosome larvae from SmBRE, SmLE, SmEG, or SmOR parasite populations. Over the course of the infection, we monitored body weight and conducted complete blood counts (CBC). On sacrifice, we measured organ weights, assessed hepatic fibrosis and granuloma size and analyzed cytokine levels to evaluate the disease progression and immunopathological changes induced by each parasite population. Host genetic background may also influence parasite-induced immunopathology. We therefore conducted these experiments using both BALB/c and C57BL/6 inbred lines. These mouse strains are commonly used in laboratory studies and differ in their innate and adaptive immune responses. BALB/c mice mount a dominant Th2 immune response to infections, while C57BL/6 mice display a Th1 bias [26, 27]. Naïve BALB/c CD4+T cells produce more IL-4 than CD4+T cells from C57BL/6 mice, which induces the proliferation of CD4+Th2 cells and lower levels of the pro-inflammatory cytokine IL-12 [28, 29].

Our results revealed that parasite genetics explained most variation in parasite traits, while immunological traits were most strongly influenced by the host. However, both parasite and host genetics affected immunopathology traits. These results provide compelling evidence for the role of parasite genetics in modulating *S. mansoni*-induced immunopathology in mouse hosts.

Methods

Ethics statement

This study was performed in accordance with the Guide for the Care and Use of Laboratory Animals of the National Institutes of Health. The protocol was approved by the Institutional Animal Care and Use Committee of Texas Biomedical Research Institute (permit no. 1420-MU).

Overview of study design

Our study design is summarized in Fig. 1, and the methodology for each stage is explained below.

Table 1 Previously investigated parasite and host traits

Authors	Parasite line	Host	Impact of parasite	Impact of host
Schistocephalus solidus				
Piecyk et al. (2019)	Sweden, Germany, Spain, Canada, Scotland, Iceland, Norway	*Gasterosteus aculeatus* from Germany (DE) and Norway (NO)	Host immune gene expression: Iceland > others *mhcII* expression in DE host: Canada < others	Parasite growth: DE > NO
Heterodera schachtii				
Nuaima and Heuer (2023)	Berklingen, Holtensen, Titz-Kalrath, Vanikum, Acholshausen, Brünnstadt	Cabbage, oilseed radish, white mustard (Germany)	Hatched eggs: Week 1 = Titz-Kalrath > Berklingen; Week 8 = Vanikum > Berklingen Penetration rate: Titz-Kalrath > Brünnstadt (cabbage); Berklingen > Holtensen (oilseed radish); Berklingen > Acholshausen(white mustard) Egg burden: Berklingen > Vanikum (cabbage); Vanikum > Titz-Kalrath (oilseed radish); Berklinge > Acholshausen (white mustard)	Penetration rate: Cabbage > white mustard > oilseed radish (several parasite lines) Egg burden: Cabbage > oilseed radish > white mustard (several parasite lines)
Schistosoma mansoni				
Anderson and Cheever (1972)	BH (Brazil), Ba (Brazil), NIH-PR (Puerto Rico), W-PR (Puerto Rico), SL (St. Lucia), Mw (Tanzania)	Albino webster mice	Egg burden: NIH-PR, Ba, SL > W-PR, BH, Mw Egg distribution in liver: NIH-PR > BH Egg distribution in colon: Mw > other Liver size: NIH-PR > others Granuloma size: PR and Mw > BH, Ba, SL	n/a
Soliman et al. (1986)	Giza (Egypt), Beni-Suef (Egypt)	Hamster	Survival: Beni-Suef > Giza Worm burden: Giza > Beni-Suef Worm size: Beni-Suef > Giza Egg size: Beni-Suef > Giza Egg burden: Giza > Beni-Suef Egg distribution in tissues: Intestine > liver > cecum > lungs for Giza vs. equal distribution for Beni-Suef	n/a
Incani et al. (2001)	YT and SM (Venezuela), BH (Brazil)	BALB/c and C57BL/6	Worm development in the host: BH, YT > SM Worm burden: BH > YT > SM Parasite sex ratio: BH > YT Egg burden: BH > YT > SM	Worm burden: BALB/c > C57BL/6 Egg burden: C57BL/6 > BALB/c
Euzébio et al. (2012)	BH, SJ and SD (Brazil)	Swiss SPF mice	Penetration rate: SJ > BH Worm burden: SD > BH Liver granuloma response: BH, SD > SJ Spleen granuloma response: SD > BH, SJ Granuloma area: SD > BH, SJ Egg size: SD > BH, SJ	n/a
Bin Dajem et al. (2008)	Egypt	BALB/c and C57BL/6	n/a	Worm burden: C57BL/6 > BALB/c Egg burden: C57BL/6 > BALB/c MDA (Malondialdehyde) levels: C57BL/6 > BALB/c

Table 1 (continued)

Authors	Parasite line	Host	Impact of parasite	Impact of host
Alves et al. (2016)	LE (Brazil)	BALB/c and C57BL/6	n/a	Granuloma area: BALB/c > C57BL/6 IL-4, IL-13: BALB/c > C57BL/6 IL10: C57BL/6 > BALB/c

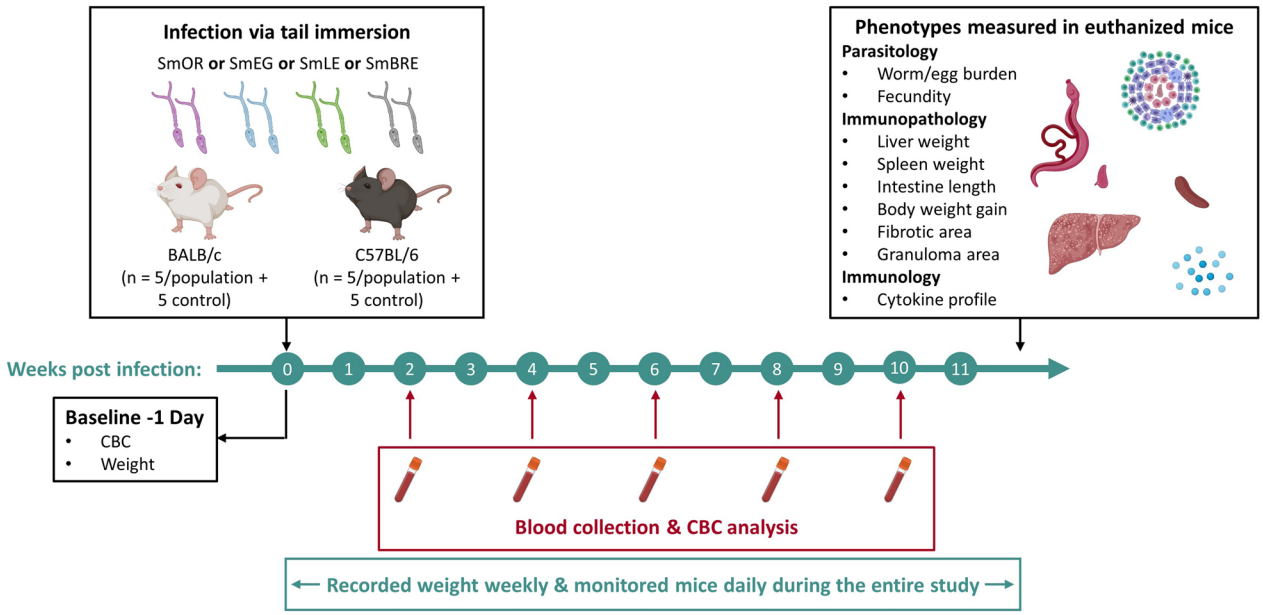

Fig. 1 Experimental timeline. We investigated the influence of parasite and host genotype on disease progression during schistosome infection in BALB/c and C57BL/6 mice. Four laboratory schistosome populations from Africa (SmEG) and the Americas (SmOR, SmLE and SmBRE) were used to infect the mice. Over a 12-week infection period, we quantified disease progression in the vertebrate host by monitoring body weight and complete blood count (CBC). Upon sacrifice, we measured multiple parasitological, immunopathological and immunological traits (see box, top right and main text)

Schistosoma mansoni parasites and mouse infection

We used SmLE (from Belo Horizonte, Brazil), SmBRE (from Recife, Brazil), SmEG (from the Theodor Bilharz Research Institute, Cairo, Egypt) and SmOR (oxamniquine resistant population homozygous for the deletion in amino acid 142 in *SmSULT-OR*) parasite populations in this study. We describe the genomic differences between the parasite populations elsewhere (Jutzeler et al., unpublished observations). In short, SmLE and SmBRE, both from Brazil, show minimal differentiation while SmOR and SmEG are strongly differentiated from one another and SmBRE/SmLE. We placed 10–20 *Biomphalaria glabrata* (Bg36 for SmLE and SmOR, BgBRE for SmBRE) and *B. alexandrina* (for SmEG) snails in beakers and shed them in artificial pond water for 2 h under light. We infected five female BALB/c and five female C57BL/6 mice (Envigo, 7–9 weeks old) per parasite population with 50 cercariae via tail immersion [30]. Control cohorts ($N=5$ per mouse line) were mock infected by placing tails in glass vials containing water but no cercariae. We conducted these infections over a 12-day period to accommodate all 50 mice but randomized cage allocation to avoid batch effects (Fig. 1).

Measuring parasitological, immunopathological and immunological traits during infection and upon sacrifice

We collected phenotypic data from each mouse during the infection period and upon euthanasia 12 weeks after the infection. We chose this time point to ensure that mice experienced both Th1 and Th2 phases of the immune response to *S. mansoni* as described in the literature [31, 32]. We categorized each trait as parasitological, immunopathological, or immunological:

Parasitological traits

Penetration rate:

We counted whole cercariae and heads that remained in the glass vial after mouse infection to calculate the penetration rate:

$$penetration\ rate = \left(1 - \frac{Cercariae + heads}{50}\right) * 100$$

Worm and egg counts in the liver and the intestine

We perfused each mouse to collect and count worms by sex [33]. To count liver eggs, the median and caudate lobes were weighed and stored in a 50-ml conical tube. The intestine was detached from the mesentery and the anus and flushed with a 1×PBS solution. We withdrew as much liquid as possible before weighing the organ and placing it in a 15-ml conical tube. Both tubes were filled with 4% KOH and stored overnight at 37°C (without agitation). The next day, we centrifuged the tubes (1500 rpm for 5 min) and removed half of the supernatant. We counted eggs in both organs in triplicate in 50–100 µl of tissue suspension and calculated the number of eggs per g of tissue as follows:

$$eggs/g\ of\ tissue = \frac{average\ egg\ counts}{organ\ weight\ (g)} \times \frac{total\ volume\ (\mu l)}{count\ volume(\mu l)}$$

Fecundity

We calculated fecundity as the total number of eggs divided by the number of female worms recovered after perfusion.

Immunopathological traits

Body weight

We weighed each mouse on the day of infection and weekly thereafter on a Mettler Toledo MS12002TS scale. We calculated the percent weight change as follows:

$$Weight\ change(\%) = \left(\frac{Weight\ after\ x\ weeks\ (g)}{Weight\ at\ baseline\ (g)}\right) \times 100 - 100$$

Liver spleen and spleen weight

We weighed each liver and spleen on a Mettler Toledo PB3002-S scale. We normalized the organ weight to account for body weight as follows:

$$Normalized\ organ\ weight(\%) = \left(\frac{Organ\ weight\ (g)}{Total\ body\ weight\ (g)}\right) \times 100$$

Intestine length

Each intestine was removed and photographed. We used the polygon tool from ImageJ 1.53k [34] to trace the intestine and return the intestine length with the built-in *Measure* command.

Liver histology to assess granuloma and fibrotic area

We stored the left frontal lobe of each liver in 10% neutral buffered formalin ($N=47$ liver samples) for further processing and embedding into paraffin. Each tissue block was cut into 4-µm sections using a Microm HM325 rotary microtome. We cut sections at 60 µm and mounted 12 sections per liver onto four slides. The slides were alternately stained with hematoxylin–eosin for quantitative analysis of granulomas or Masson's trichrome to detect fibrosis due to collagen deposition [35]. All slides were scanned with the Zeiss Axio Scan.Z1 whole-slide scanner at a resolution of 0.22 µm/pixel. We analyzed sections that were at least 120 µm apart using HALO® software (v3.4, Indica Labs). We annotated and quantified the area of individual granulomas (16–44/liver) surrounding a single schistosome egg, recording 118–152 granulomas for each experimental group. To assess fibrotic area, we trained HALO's Area Quantification tool (v2.3.1) on the different trichrome dyes (blue, red, brown). This tool automatically detects pixels of an assigned color and calculates the total area stained with each dye.

Immunological traits

Complete blood count (CBC) with differential

We obtained CBC profiles with differential to measure the number of each white blood cell type from individual mice before infection and then bi-weekly until week 10. Briefly, we used a 4- or 5-mm lancet (Goldenrod Animal Lancet, Medipoint, Mineola, NY) to puncture the submandibular vein and collected the blood in an EDTA tube (Microtainer, Becton Dickenson). We injected mice with 50–100 µl 5% saline solution to replace fluids and promote recovery. Blood was analyzed using a ProCyte Dx Hematology Analyzer (IDEXX Laboratories, Inc., Westbrook, ME).

Cytokine assay

We collected 100–200 µl of blood by cardiac puncture after euthanasia but before perfusion. We stored the blood in a microcentrifuge tube for 20–23 min at room temperature before spinning the tube at 2000×*g* for 10 min. We collected the serum fraction in a new tube and placed it on dry ice until permanent storage at −80 °C. We used the LEGENDplex™ Mouse Th1/Th2 Cytokine Panel V03 (BioLegend®, San Diego, CA) to simultaneously quantify eight

cytokines (IFN-γ, IL-5, TNF-α, IL-2, IL-6, IL-4, IL-10 and IL-13) secreted by Th1 and/or Th2 cells. Following the manufacturer instructions, we diluted 12.5 µl of serum with 12.5 µl of assay buffer and prepared reactions in 96-well V-bottom plates. We transferred the reactions to sterile snap cap tubes (VWR) and read the samples on a BD Symphony Analyzer. The analysis was conducted using LEGENDplex™ Cloud-based Data Analysis Software (https://legendplex.qognit.com/).

Statistical analysis

Trait-by-trait analyses

We performed all statistical analyses and plotted graphs using R software (v4.2.0) and package *rstatix v0.7.2* [36, 37]. We excluded the control group from statistical analyses examining differences between parasite populations in immunopathology. In addition, we normalized all traits by penetration rate to account for differences between individual mice. For normally distributed data (Shapiro test, $p > 0.05$) with homogeneous variance (Bartlett test, $P > 0.05$), we used one-way ANOVA followed by the Tukey HSD post hoc test. For non-normally distributed data, we applied the Kruskal-Wallis test followed by Dunn's post hoc test or the Friedman test followed by Conover's post hoc test for longitudinal analysis. We adjusted *P*-values for multiple comparisons using the Benjamini-Hochberg method and considered these significant when $P < 0.05$ [38]. To make comparisons between hosts, we performed Wilcoxon rank-sum tests (non-parametric) or Student's t-tests (parametric).

General linear modeling (GLM)

We suspected that some differences in immunopathology may be explained by differences in egg counts among parasite populations. We conducted generalized linear modeling (GLM) of all phenotypes using the function glm() from the *stats* R package. We assessed the fit of linear models by examining the distribution of residuals, quantile-quantile, scale-location plots and Bayesian information criterion (BIC) and normalized the dependent variable with log (liver weight, fibrosis, intestine length, granuloma area, all cytokine data, lymphocytes, reticulocytes) or square root (spleen weight, eosinophils, neutrophils, monocytes) transformation to improve the fit of the model when applicable [39]. The following model showed the best fit for all parasitological, immunopathological and cytokine measures except liver weight:

$$phenotype \sim parasite\ population * host\ strain + total\ egg\ counts$$

We used an interaction model exclusively for liver weight:

$$phenotype \sim parasite\ population * hoststrain * total\ egg\ counts$$

To account for baseline values, we used the following model for CBC data:

$$phenotype \sim parasite\ population * host\ strain + total\ egg\ counts + baseline\ counts$$

Contribution of parasite and host to immunopathology

To determine effect size of parasite population and host genotype, we first log-transformed non-normally distributed data and then used the R function aov() from the *stats* package to perform an ANOVA test for each parameter before calculating effect sizes with the eta_squared() function from the *effectsize v0.8.6* package for R [40].

Results

Parasitological phenotypes

Penetration rates

We measured parasite penetration rates by counting whole cercariae and heads that remained in the glass vial after mouse infection [41]. We found no significant differences between experimental groups (Fig. 2A; Kruskal-Wallis; BALB/c: $H = 4.15$, $df = 3$, $P = 0.246$; C57BL/6: H 2.5, $df = 3$, $P = 0.475$; Wilcoxon test to compare hosts; BRE: $W = 13$, $P = 1$, EG: $W = 11.5$, $P = 1$, LE: $W = 6.5$, $P = 0.984$, OR: $W = 9$, $P = 1$).

Host survival

All C57BL/6 mice survived throughout the study period. However, we sacrificed three BALB/c mice because of severe disease progression during the study (SmLE: days 54 and 74, SmEG: day 83), and two BALB/c mice died spontaneously without visual symptoms but infection-associated weight loss (SmEG: day 63, SmOR: day 75). Details about these mice can be found in Additional File 1: Table S1.

Worm and egg burden

On perfusion, we observed significant variation in worm burden among both mouse hosts infected with the four parasite populations (Fig. 2B; ANOVA; BALB/c: $F_{(3, 16)} = 4.34$, $P = 0.020$; C57BL/6: $F_{(3, 16)} = 3.99$, $P = 0.027$). SmEG caused significantly higher worm burden than SmBRE in both mouse hosts and SmOR in BALB/c mice. Liver egg burden varied significantly in both BALB/c and C57BL/6 mice infected with the four parasite populations (Fig. 2C; ANOVA; BALB/c: $F_{(3,}$

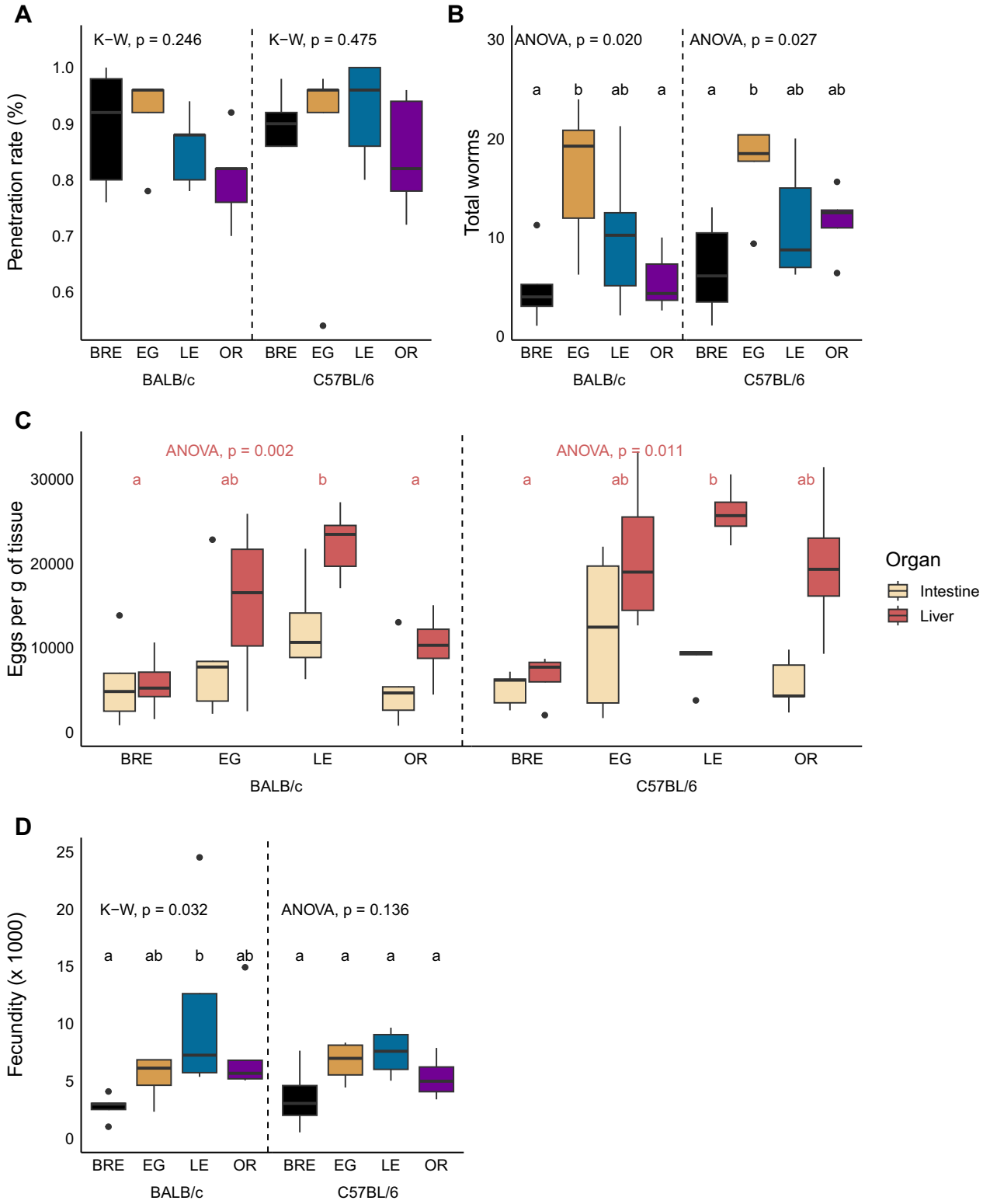

Fig. 2 Parasitological outcome is driven by parasite rather than host genotype. Box and whisker plots showing **A** cercarial penetration rate, **B** worm burden, **C** liver and intestine egg counts and **D** fecundity for infections with SmBRE, SmEG, SmLE and SmOR in BALB/c (left) and C57BL/6 mice (right). Parasite populations were compared separately for each host strain. Different letters indicate comparisons that are statistically different as analyzed using Kruskal-Wallis (K-W) followed by Dunn's or ANOVA followed by Tukey HSD post hoc test. Use of ANOVA or Kruskal-Wallis is shown at the top of each graph. For (C), stats are shown for liver eggs only. Host differences were not significant in any of the figures

$_{15)}$ = 7.96, P = 0.002; C57BL/6: $F_{(3, 12)}$ = 5.81, P = 0.011). SmLE-infected mice had the highest liver egg burden, while SmBRE caused the lowest burden in both mouse strains. Comparisons between host strains revealed no significant differences in terms of parasite and egg burden.

Tissue distribution of eggs

Visual inspection of Fig. 2C suggests differences in tissue distribution of eggs for the four parasite populations. We therefore examined tissue tropism by comparing egg burden in liver and gut. However, the distribution of eggs in SmEG, SmLE, SmOR and SmBRE-infected mice was not significantly different in the tissues or influenced by host genotype (Fig. 2C). We conducted a separate analysis comparing the ratio between liver and intestine eggs in individual mice, but this similarly revealed no significant differences (Additional file 2: Fig. S1).

Fecundity

Fecundity was significantly higher in BALB/c mice that were infected with SmLE compared to SmBRE (Fig. 2D; Kruskal-Wallis, H = 8.82, df = 3, P = 0.032). We did not detect an impact of host genotype on worm fecundity.

Parasite genotype and parasite burden impact tissue damage

Next, we analyzed immunopathological phenotypes in the infected mice. To focus on differences between parasite populations rather than host infection status, we excluded the control group from the following statistical analyses.

Mouse growth

Schistosome-infected mice typically experience weight gain during the early stages of the infection [42–44]. Schistosome eggs are usually excreted through the intestine but can migrate to other tissues and induce hepatosplenomegaly in both humans and mice [45], which may contribute to the observed increase in body weight. Overall, infected C57BL/6 mice gained more weight than BALB/c mice, though this difference was not significant at the end of the 12-week period. However, SmLE-infected BALB/c mice exhibited a significantly reduced weight gain compared to BALB/c mice infected with SmEG and SmOR, while BALB/c mice infected with SmOR gained more weight compared to their counterparts infected with SmBRE or SmLE (Fig. 3A; Friedman test; BALB/c: $\chi 2$ = 27.2, df = 3, P < 0.001). We did not detect any significant differences between the infected C57BL/6 mice (Fig. 3A; Friedman test; C57BL/6: $\chi 2$ = 1.3, df = 3, P = 0.729).

Liver and spleen weight and intestine length

All infected mice exhibited hepatosplenomegaly compared to uninfected control groups. Livers of SmBRE infected mice were significantly smaller than livers of all other infected mice regardless of the host strain (Fig. 3B; BALB/c: ANOVA, $F_{(3, 16)}$ = 9.00, P = 0.001; C57BL/6: Kruskal-Wallis, H = 10.7, df = 3, P = 0.013). Similarly, mice infected with SmBRE had a significantly reduced spleen mass compared to mice infected with SmEG (in BALB/c), SmOR (in C57BL/6) and SmLE (Fig. 3C; BALB/c: Kruskal-Wallis, H = 8.12, P = 0.044; C57BL/6: ANOVA, $F_{(3, 16)}$ = 5.55, P = 0.008). Intestine length was not significantly different between mouse strains (Additional file 3: Fig. S2).

Fibrotic area and granuloma size

All infected mice had an increase of fibrotic liver tissue, with SmBRE causing less fibrosis than other parasite populations, though this difference was only statistically significant compared with C57BL/6 mice infected with SmLE (Fig. 3D; ANOVA; BALB/c: $F_{(3, 13)}$ = 2.26, P = 0.129; C57BL/6: $F_{(3,16)}$ = 4.00, df = 3, P = 0.027). Fibrotic area did not differ between the host strains.

Contrary to other reports that noted increased granuloma area in BALB/c mice [46, 47], we measured larger granulomas in infected C57BL/6 mice (Fig. 3E; Wilcoxon test; EG: W = 6021, P = 0.038; LE: W = 4703,

(See figure on next page.)

Fig. 3 Impact of parasite and host on mouse immunopathology. **A** Longitudinal plots of weight gain in mice infected with the four parasite populations (solid lines) and uninfected controls (dotted lines). Means shown with standard error. **B** Liver weight or **C** spleen weight from euthanized BALB/c (left) and C57BL/6 mice (right) infected with the four parasite populations or uninfected controls. Photos (right) show representative organ samples from C57BL/6 mice infected with the four parasite populations and the control group for reference. Differences between hosts were not significant. **D** Fibrotic area and **E** granuloma area measured from liver sections. For all box plots, statistical comparisons are between infected groups only. Comparisons between parasite populations were conducted for each host strain separately. Different letters mean groups are significantly different in comparisons using Kruskal-Wallis (K–W) followed by Dunn's or ANOVA followed by Tukey HSD post hoc test. Differences between BALB/c (left) and C57BL/6 mice (right) in the pathology traits were calculated with Wilcoxon rank-sum or Student's t-test and are shown by: $^{\#}P$ < 0.05, $^{\#\#}P$ < 0.01, $^{\#\#\#}P$ < 0.001

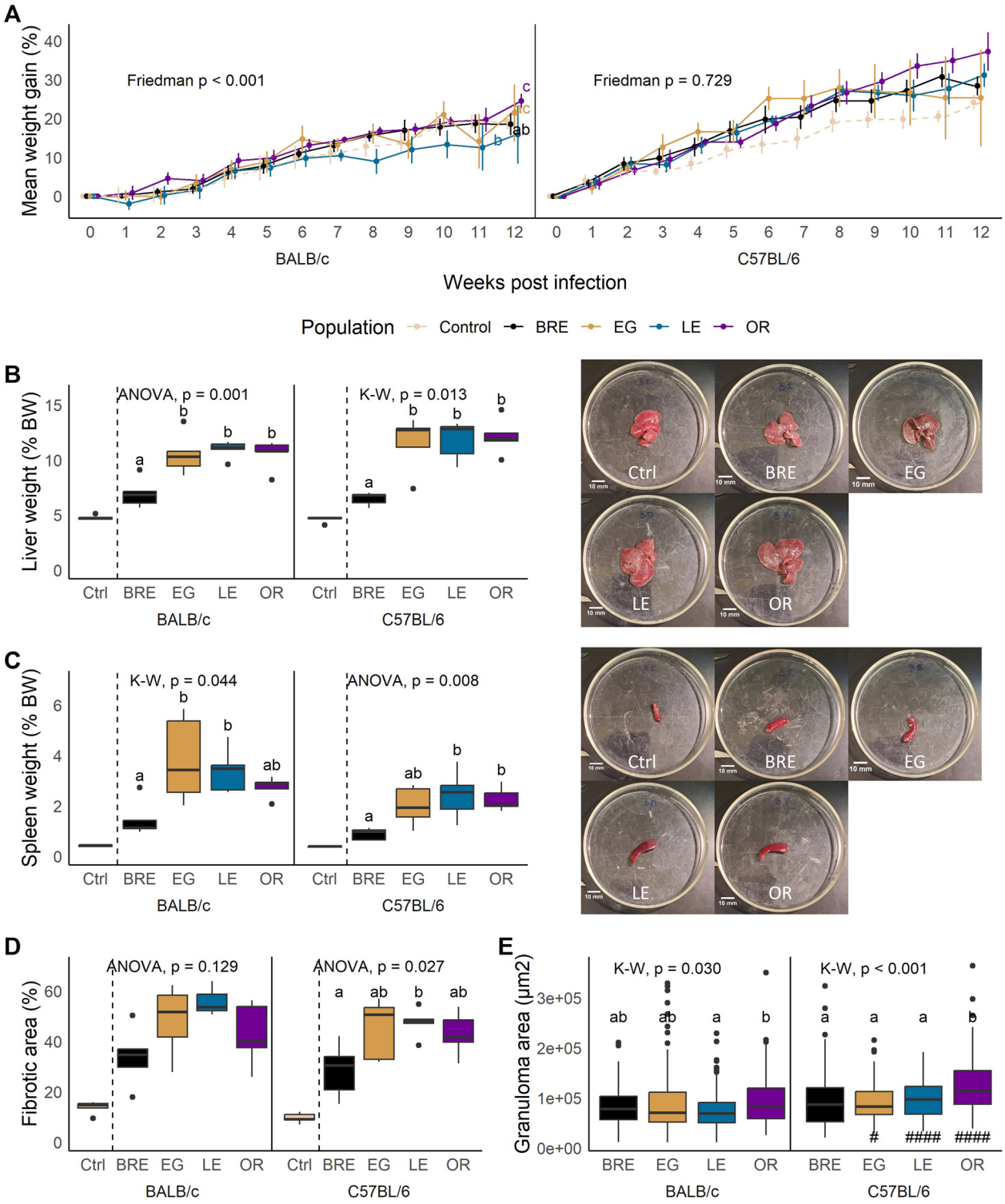

Fig. 3 (See legend on previous page.)

$P < 0.001$, OR: $W = 5095$, $P < 0.001$). In addition, infection of C57BL/6 mice with SmOR resulted in the formation of larger granulomas compared to all other parasite populations while the same infection resulted in bigger granulomas compared to SmLE-infected BALB/c

Table 2 Generalized linear model output for all traits

Characteristic	Liver weight[2,4]			Spleen weight[3]			Intestine length[2]			Fibrotic area[2]			Granuloma area[2]		
	Beta	95% CI[1]	*P*-value	Beta	95% CI[1]	*P*-value	Beta	95% CI[1]	*P*-value	Beta	95% CI[1]	*P*-value	Beta	95% CI[1]	*P*-value
Parasite			< 0.001*			< 0.001*			0.2			0.07			0.2
BRE	–	–		–	–		–	–		–	–		–	–	
EG	0.84	0.57, 1.1		0.67	0.36, 0.98		−0	−0.11, 0.06		0.45	0.08, 0.82		7,005	−11,113, 25,123	
LE	0.44	0.06, 0.82		0.39	0.06, 0.72		0.07	−0.02, 0.16		0.39	0.00, 0.77		4,431	−14,421, 23,282	
OR	0.29	0.02, 0.56		0.33	0.06, 0.61		0.02	−0.05, 0.09		0.12	−0.19, 0.44		17,068	1,867, 32,269	
Host			0.3			0.074			0.004*			0.089			0.8
BALB/c	–	–		–	–		–	–		–	–		–	–	
C57BL/6	−0.2	−0.49, 0.17		−0.3	−0.56, 0.03		−0.1	−0.18, −0.03		−0.3	−0.62, 0.04		−1,904	−17,978, 14,170	
Total eggs	0	0.00, 0.00	0.011*	0	0.00, 0.00	0.004*	0	0.00, 0.00	0.001*	0	0.00, 0.00	0.11	−0.11	−0.59, 0.37	0.7
Parasite x host			< 0.001*			0.04*			0.5			0.8			0.5
EG x C57BL/6	−0.6	−1.0, −0.17		−0.5	−0.95, −0.10		0.03	−0.08, 0.14		0.01	−0.49, 0.52		−6,516	−31,085, 18,053	
LE x C57BL/6	−0.6	−1.3, 0.14		−0.1	−0.56, 0.29		−0	−0.14, 0.08		0.1	−0.41, 0.60		−10,018	−34,542, 14,506	
OR x C57BL/6	0.37	−0.13, 0.87		0.04	−0.38, 0.46		0.06	−0.05, 0.16		0.23	−0.25, 0.70		−18,619	−41,720, 4,483	

*Statistically significant, [1] CI = confidence interval, [2] log transformed dependent variable, [3] square root transformed dependent variable, [4] different model due to better fit evaluated by BIC (see Methods)

mice (Fig. 3E; Kruskal-Wallis; BALB/c: H = 8.93, df = 3, $P = 0.030$; C57BL/6: H = 36.5, df = 3, $P < 0.001$).

Does parasite genotype and/or egg burden impact organ pathology?

We used generalized linear modeling (GLM) to examine the effects of parasite population, host strain, total egg burden and host-parasite interactions (Table 2). Liver weight, spleen weight and intestine length were all heavily influenced by the total egg burden. However, we also identified a significant effect of parasite population on both liver and spleen weight. In turn, the host strain emerged as a significant factor affecting intestine length. Intriguingly, the GLM analysis unveiled a contribution approaching significance of the parasite population to fibrosis, confirming the results from the trait-by-trait analysis (Fig. 3D). We also found that host-parasite interactions significantly influenced liver and spleen weight but not other traits examined. However, this was significant for the interaction model (liver weight) and square root transformed data (spleen weight) only.

Host genotype is associated with the immunological response to infection

Complete blood counts

To monitor the immune response during infection, we conducted a complete blood count (CBC) with differential every 2 weeks. As anticipated with helminths, eosinophilia was observed in all infected mice [48], though we did not detect any significant differences between parasite populations in either host strain (Fig. 4A, Friedman; BALB/c $\chi2 = 3.2$, df = 3, $P = 0.362$; C57BL/6: $\chi2 = 2.2$, df = 3, $P = 0.532$). We observed an increase in basophils in SmEG-infected C57BL/6 mice past the 6-week mark, though it was not significant according to a Friedman test (Fig. 4B; Friedman; BALB/c: $\chi2 = 1$, df = 3, $P = 0.801$; C57BL/6: $\chi2 = 6.2$, df = 3, $P = 0.102$). We observed the same outcome with lymphocytes (Fig. 4C; Friedman;

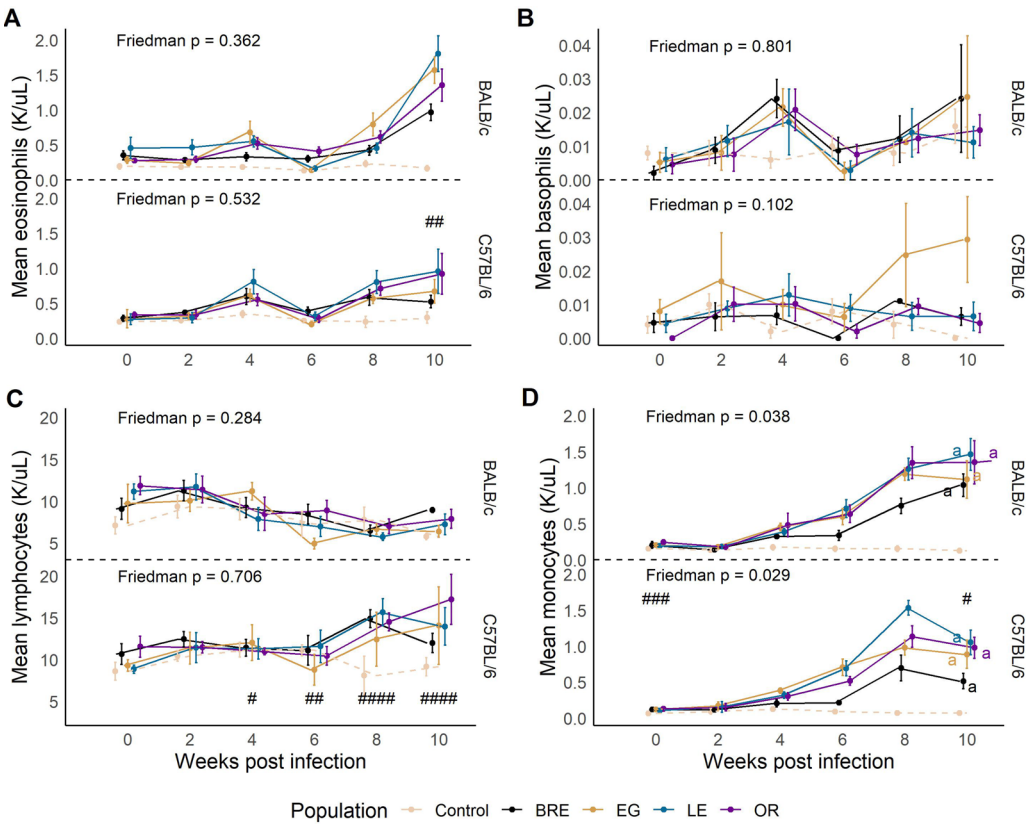

Fig. 4 White blood cells are influenced by host background. Longitudinal data of **A** eosinophil, **B** basophil, **C** lymphocyte and **D** monocyte levels in BALB/c (top) and C57BL/6 mice (bottom) infected with the four infected parasite populations (solid lines) or uninfected controls (dotted lines). For all plots, statistical comparisons are between infected groups only. Mice with missing data points were excluded from the analysis. Groups with different letters and separated by host strain are significantly different (Friedman's test followed by Conover's post hoc test). #$P < 0.05$, ##$P < 0.01$, ###$P < 0.001$: values are significantly different between infected (parasite populations combined) host strains using Wilcoxon rank-sum test

Table 3 Generalized linear model output for CBC

Characteristic	Eosinophils[3]			Neutrophils[3]			Monocytes[3]			Lymphocytes[2]			Basophils			Reticulocytes[2]		
	Beta	95% CI[1]	P-value	Beta	95% CI[1]	*P*-value	Beta	95% CI[1]	*P*-value	Beta	95% CI[1]	*P*-value	Beta	95% CI[1]	*P*-value	Beta	95% CI[1]	*P*-value
Parasite			0.11			0.7			> 0.9			0.4			0.2			0.9
BRE	–	–		–	–		–	–		–	–		–	–		–	–	
EG	0.28	0.02, 0.54		−0.1	−0.59, 0.33		0.02	−0.23, 0.27		−0.3	−0.71, 0.13		0	−0.03, 0.02		−0.2	−0.64, 0.29	
LE	0.27	−0.01, 0.54		−0.3	−0.76, 0.18		0	−0.26, 0.26		−0.3	−0.68, 0.17		−0	−0.05, 0.00		−0.1	−0.51, 0.41	
OR	0.08	−0.14, 0.30		−0.1	−0.50, 0.27		0.04	−0.17, 0.25		−0.3	−0.62, 0.09		−0	−0.03, 0.01		0	−0.39, 0.38	
Host			0.03*			0.2			0.007*			0.3			0.2			0.3
BALB/c	–	–		–	–		–	–		–	–		–	–		–	–	
C57BL/6	−0.3	−0.49, −0.03		−0.3	−0.69, 0.17		−0.3	−0.58, −0.09		0.21	−0.16, 0.58		−0	−0.04, 0.01		−0.2	−0.63, 0.17	
Total eggs	0	0.00, 0.00	0.3	0	0.00, 0.00	0.055	0	0.00, 0.00	0.015*	0	0.00, 0.00	0.8	0	0.00, 0.00	0.021*	0	0.00, 0.00	0.002*
Baseline	−0.1	−0.62, 0.36	0.6				−0.2	−1.3, 0.88	0.7	0.01	−0.04, 0.06	0.8	0.27	−1.1, 1.6	0.7	0	0.00, 0.00	0.4
Parasite x host			0.11			0.5			0.8			0.14			0.9			0.4
EG x C57BL/6	−0.3	−0.61, 0.10		−0.1	−0.89, 0.61		0.08	−0.26, 0.42		0.42	−0.15, 0.98		0.01	−0.03, 0.04		0.26	−0.35, 0.87	
LE x C57BL/6	−0.3	−0.59, 0.07		0.08	−0.51, 0.68		0.12	−0.20, 0.45		0.37	−0.18, 0.92		0.01	−0.02, 0.05		0.18	−0.41, 0.77	
OR x C57BL/6	0.08	−0.26, 0.42		0.33	−0.27, 0.92		0.13	−0.19, 0.45		0.63	0.10, 1.2		0	−0.03, 0.04		0.52	−0.05, 1.1	

*Statistically significant, [1]CI = confidence interval, [2]log-transformed dependent variable, [3]square root transformed dependent variable

BALB/c: $\chi2=3.8$, df = 3, $P=0.284$; C57BL/6: $\chi2=1.4$, df = 3, $P=0.706$). Both monocyte (Fig. 4D; Friedman; BALB/c: $\chi2=8.4$, df = 3, $P=0.038$; C57BL/6: $\chi2=1.4$, df = 3, $P=0.029$) and neutrophil levels (Additional file 4: Fig. S3A) exhibited an upward trend in infected mice, which resulted in significant Friedman tests. Because of *P*-value adjustment, however, we did not detect significant differences between parasite populations.

As we did not observe significant differences between parasite populations in the CBC analysis, we grouped infected mice together to compare host strains. BALB/c mice had more circulating eosinophils in the blood after 10 weeks of infection than their C57BL/6 counterparts (Fig. 4A; Wilcoxon; Week 10: W = 305, $P=0.00163$). In addition, lymphocyte production varied between the host strains, increasing in C57BL/6 mice after 6 weeks (Fig. 4C; Wilcoxon; Week 4: W = 91, $P<0.0128$; Week 6: W = 71, $P<0.00208$; Week 8: W = 1, $P<0.001$; Week 10: W = 25, $P<0.001$). Monocytes differed between the infected hosts at the beginning and end of the infection (Fig. 4D; Wilcoxon; Baseline: W = 318, $P<0.001$; Week 10: W = 266, $P=0.0387$), whereas neutrophil levels varied significantly between the hosts at baseline and week 4 (Additional file 4: Fig. S3A).

We anticipated a decrease in hematocrit in infected animals, because schistosome parasites feed on blood [49]. Surprisingly, none of the mice exhibited signs of anemia throughout the infection period (Additional file 4: Fig. S3B), though we observed a significant difference in hematocrit levels between SmOR and other parasite populations in both mouse hosts. Furthermore, we noticed a significant increase in reticulocytes in the later stage of infection (Additional file 4: Fig. S3C).

We used GLM to assess contributions of the parasite, host and egg burden, incorporating baseline values into the model for week 10 CBC measurements (Table 3). Mouse line was the dominant factor for eosinophils and monocytes but not for lymphocyte production. In addition, total egg burden significantly impacted monocyte, basophil and reticulocyte levels. We did not see any impact of parasite genotype or host-parasite interactions.

Cytokines

We quantified eight Th1/Th2 associated cytokines in serum collected at week 12. Our analysis showed no significant differences between parasite populations for any of the measured cytokines. However, we observed significant variations between the different host strains. First, IFN-γ levels were significantly elevated in BALB/c mice compared to C57BL/6 (Fig. 5A; Wilcoxon; BR, EG, LE: W = 25, $P=0.011$; OR: W = 20, $P=0.016$). In contrast, C57BL/6 mice produced more TNF-α in response to schistosome infection than BALB/c mice (Fig. 5B; Wilcoxon; BRE: W = 0, $P=0.032$; EG: W = 5, $P=0.151$; LE: W = 2, $P=0.042$, OR: W = 1, $P=0.042$). Finally, IL-6 was significantly higher in BALB/c mice, but only when they were infected with SmEG or SmOR (Fig. 5E; Wilcoxon; EG: W = 24, $P=0.032$; OR: W = 20, $P=0.032$).

Host background did not significantly affect the production of cytokines IL-2, IL-4, IL-5, IL-10 and IL-13 (Fig. 5C, D, Additional file 5: Fig. S4A-C), but they exhibited substantial variation among all groups, with outcomes differing based on host-parasite interactions. For instance, SmOR infection led to an increase of IL-4, IL-5 and IL-10 in BALB/c but not in C57BL/6 mice. Similarly, cytokines IL-4 and IL-10 were higher in BALB/c than C57BL/6 mice infected with SmEG. Conversely, SmLE infection resulted in elevated levels of IL-2, IL-4, IL-5 and IL-6 and a decrease in IL-13 in C57BL/6 but not in BALB/c mice. SmBRE led to higher secretion of IL-6 in BALB/c and lower production of IL-10 and IL-13 in C57BL/6 mice.

GLM analysis supported a significant impact of host strain on IFN-γ, TNF-α and IL-6 secretion (Table 4). We also revealed that IL-5 production was significantly impacted by host-parasite interactions. However, we observed no direct impact of parasite population on cytokine levels, which was consistent with the trait-by-trait analysis.

Contribution of parasite population and host strain to infection phenotypes

Our trait-by-trait and GLM analyses suggest that parasitological traits tend to be determined by parasite genetics, while immunological phenotypes (CBC and cytokines) tend to be more affected by host genotype. We used effect size measures to directly partition the impact of parasite population, host genotype and host-parasite interactions on infection phenotypes. We categorized all phenotypes into parasitological, immunopathological or immunological traits. We found that parasite population had a large and significant effect on three out of four parasitological traits, whereas host strain had a strong effect on seven of 13 immunological traits (Fig. 6). Immunopathological traits were impacted by both host (three of six traits) and parasite (three of six traits). This analysis also identified significant host-parasite interaction effects for IL-5 secretion, consistent with the GLM analysis.

Discussion

Parasite population effects on immunopathology

Egg burden is measured in epidemiological surveys because it is an important predictor of immunopathology in schistosomiasis [50–52]. Parasite genotype contributes to immunopathology in two ways in our experiments. First, we see significant differences between

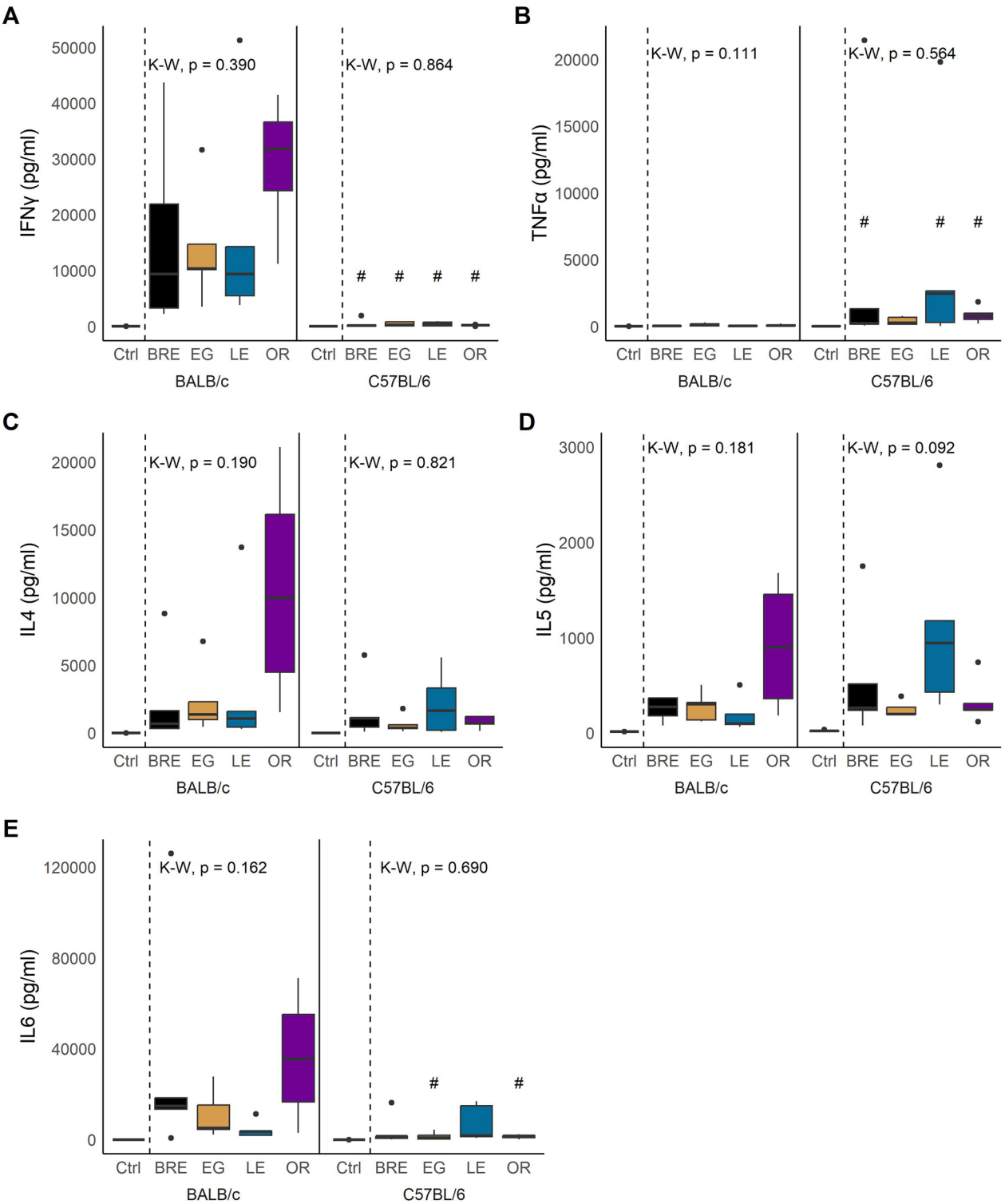

Fig. 5 Cytokine production in response to schistosome infection. Box and whisker plots showing cytokine production of **A** IFN-γ, **B** TNF-α, **C** IL-4, **D** IL-5 and **E** IL-6 in BALB/c (left) and C57BL/6 mice (right) infected with the four parasite populations or uninfected controls. For all plots, statistical comparisons are separated by host strain and between infected groups only using Kruskal-Wallis (K-W) followed by Dunn's post hoc test. #$P < 0.05$, ##$P < 0.01$, ###$P < 0.001$: values are significantly different between host strains as calculated by Wilcoxon rank-sum test

Table 4 Generalized linear model output for cytokine data

Characteristic	IFN-γ[2]			TNF-α[2]			IL2[2]		
	Beta	95% CI[1]	*P*-value	Beta	95% CI[1]	*P*-value	Beta	95% CI[1]	*P*-value
Parasite			0.6			0.11			0.085
BRE	–	–		–	–		–	–	
EG	0.64	−0.84, 2.1		2	0.14, 3.9		1	−0.18, 2.3	
LE	0.69	−0.90, 2.3		0.35	−1.7, 2.4		−0.3	−1.6, 1.1	
OR	0.9	−0.49, 2.3		1.3	−0.44, 3.1		0.9	−0.25, 2.1	
Host			< 0.001*			0.004*			0.9
BALB/c	–	–		–	–		–	–	
C57BL/6	−4.7	−6.0, −3.3		2.6	0.83, 4.4		0.1	−1.1, 1.3	
Total eggs	0	0.00, 0.00	0.11	0	0.00, 0.00	0.6	0	0.00, 0.00	0.7
Parasite x host			0.3			0.2			0.2
EG x C57BL/6	1.1	−0.90, 3.2		−1.4	−4.0, 1.2		−0.1	−1.7, 1.6	
LE x C57BL/6	1.4	−0.59, 3.4		1.6	−0.93, 4.2		1.5	−0.20, 3.1	
OR x C57BL/6	−0.3	−2.4, 1.8		−0.2	−2.8, 2.4		−0.2	−1.9, 1.5	

Characteristic	IL4[2]			IL5[2]		
	Beta	95% CI[1]	*P*-value	Beta	95% CI[1]	*P*-value
Parasite			0.2			0.2
BRE	–	–		–	–	
EG	1.2	−0.57, 3.0		0.25	−0.84, 1.3	
LE	0.8	−1.1, 2.7		−0.4	−1.5, 0.82	
OR	1.8	0.15, 3.5		0.94	−0.09, 2.0	
Host			0.4			> 0.9
BALB/c	–	–		–	–	
C57BL/6	−0.7	−2.4, 0.96		0.03	−1.0, 1.1	
Total eggs	0	0.00, 0.00	0.2	0	0.00, 0.00	> 0.9
Parasite x host			0.4			0.005*
EG x C57BL/6	−0.5	−3.0, 2.0		−0.2	−1.7, 1.3	
LE x C57BL/6	0.85	−1.6, 3.3		1.9	0.36, 3.3	
OR x C57BL/6	−1.4	−3.9, 1.1		−0.9	−2.4, 0.68	

Characteristic	IL6[2]			IL10[2]			IL13[2]		
	Beta	95% CI[1]	*P*-value	Beta	95% CI[1]	*P*-value	Beta	95% CI[1]	*P*-value
Parasite			0.7			0.2			0.11
BRE	–	–		–	–		–	–	
EG	−0.1	−2.0, 1.9		1.3	−0.16, 2.7		1.6	0.27, 3.0	
LE	−0.9	−2.9, 1.2		−0.1	−1.6, 1.4		1.4	−0.12, 2.8	
OR	0.38	−1.4, 2.2		0.64	−0.70, 2.0		0.89	−0.40, 2.2	
Host			< 0.001*			> 0.9			0.2
BALB/c	–	–		–	–		–	–	
C57BL/6	−3.1	−4.9, −1.3		0.05	−1.3, 1.4		0.87	−0.42, 2.2	
Total eggs	0	0.00, 0.00	0.6	0	0.00, 0.00	0.8	0	0.00, 0.00	0.2
Parasite			0.066			0.4			0.3
EG x C57BL/6	0.94	−1.7, 3.5		−1.4	−3.3, 0.54		−1.5	−3.4, 0.34	
LE x C57BL/6	3.2	0.61, 5.8		0.03	−1.9, 2.0		−1.2	−3.0, 0.72	
OR x C57BL/6	0.15	−2.5, 2.8		−1	−3.0, 0.97		−0.3	−2.2, 1.7	

*Statistically significant, [1]CI = confidence interval, [2]log-transformed dependent variable

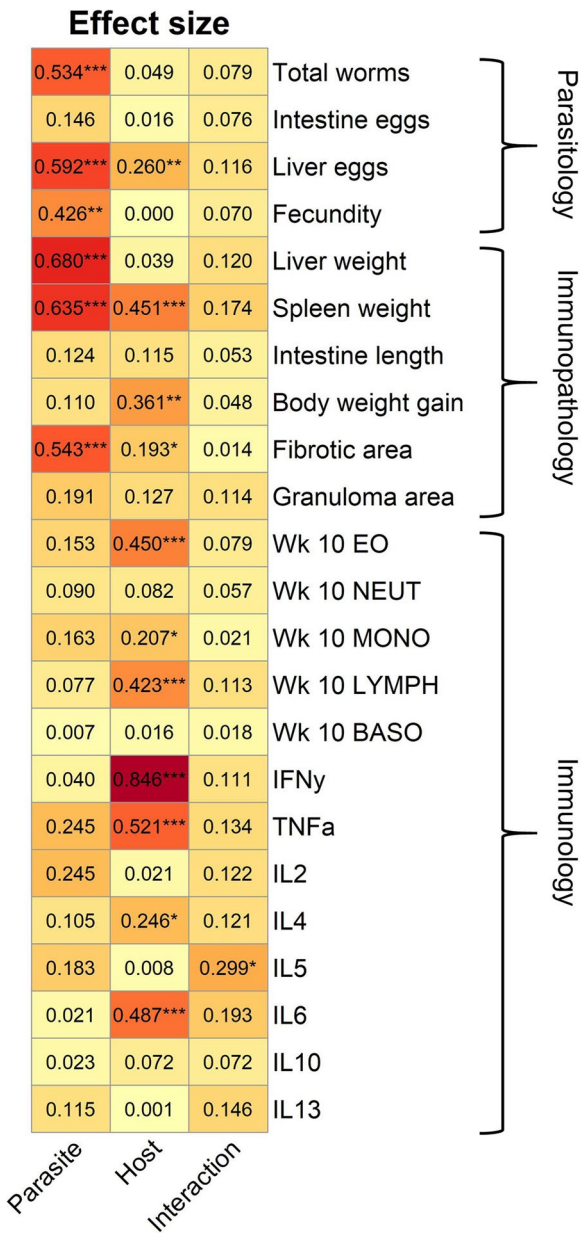

Fig. 6 Effect size by parasite and host genotype on disease parameters. Heatmap showing effect size measures (eta squared) as calculated by ANOVA. Parasite includes the four parasite populations, host includes both mouse strains, and interactions applies to the interaction between the two. Traits are organized in rows and assigned to the parasitology, immunopathology, or immunology category. *$P < 0.05$, **$P < 0.01$, ***$P < 0.001$: values are significant per ANOVA result

parasite populations in worm burden and fecundity. These jointly contribute to large differences in egg burden between parasite populations and impact liver and spleen weight and fibrosis. However, our GLM analysis (Table 2), which accounted for parasite population, host strain and egg burden, attributed a significant impact of parasite population to liver and spleen weight. While egg burden contributed to variation in these traits, parasite population also had a significant independent impact, suggesting that this is a parasite intrinsic factor and not merely related to variation in egg production observed in the different parasite populations. This is clearly shown by examining correlations between egg burden and organ weight (Additional file 6: Fig. S5).

This study confirms and extends our previous findings from studies of two Brazilian populations, SmBRE and SmLE, that show striking differences in cercarial shedding and sporocyst growth in the intermediate snail host [18, 19, 53]. These two parasite populations also showed the most extreme phenotype differences during infection in the vertebrate host. Despite comparable penetration success, we counted fewer worms and eggs and calculated lower fecundity in mice infected with SmBRE. Additionally, parameters such as liver weight, spleen weight and fibrotic area were also lower in SmBRE-infected mice compared to the other schistosome populations characterized in the present study. We have previously demonstrated that fibrotic area and granuloma size were reduced in mice infected with parasite progeny from SmBRE and SmLE genetic crosses selected for low or high cercarial shedding from the aquatic snail [19]. While the experimental design in this study was rather different, we saw comparable differences in fibrotic area (lower in SmBRE than in SmLE), although granuloma size was unaffected. These observations underscore the profound impact of parasite factors on multiple phenotypes including immunopathology.

Host genetic influences on susceptibility and immune profiles during infection

We did not detect differences in susceptibility and parasite fecundity between the mouse host strains. This supports findings from Alves et al. [46] who used SmLE and found no effect of mouse genetic background on worm and egg burden (Table 1). However, this is inconsistent with reports by Incani et al. [23], who documented higher worm but lower egg burden in BALB/c compared to C57BL/6 mice using Venezuelan and Brazilian *S. mansoni* populations, and Bin Dajem et al. [54], who found increased worm burden in C57BL/6 hosts with an Egyptian parasite. These differences could be explained by (i) the number of cercariae used for the infection (Alves: 30, Incani: 60, Bin Dajem: 100), (ii) the method of infection (tail immersion vs. abdominal skin), (iii) statistical methods (log transformation vs. non-parametric tests), (iv) duration of the study or (v) even genetic variation in the mouse colonies maintained at the different institutions [55].

IFN-γ, TNF-α, IL-6, monocyte and eosinophil levels were strongly influenced by host genotype as indicated by GLM and ANOVA analyses. This aligned with our expectations since C57BL/6 and BALB/c mice are known to induce different immune responses to many pathogens and are typically described as IFN-γ high/IL-4 low and IFN-γ low/IL-4 high responders respectively [26]. We observed comparable levels of IL-4 in BALB/c and C57BL/6 mice but significantly increased IFN-γ (a known antifibrogenic agent) levels in infected BALB/c mice [56]. We hypothesize that this outcome represents hyperproduction in BALB/c mice, inducing protective immunity in response to schistosome infection [31, 57]. This could prevent BALB/c mice from mounting a potent type 2 immune response, impact granuloma formation and explain the mortality we observed in BALB/c and not in C57BL/6 mice [32, 58, 59]. However, we opted to measure cytokines 12 weeks post-infection, a time at which mice have progressed through both Th1 and Th2 associated phases and entered the chronic phase of infection [31, 32]. While it is likely that host differences could be observed earlier in the infection, our selection of this time point may have led us to overlook potential differences between parasite populations at earlier stages of infection.

We observed larger granulomas, which are predominantly driven by a type 2 immune response, in C57BL/6 mice [45, 48, 60]. In contrast, Alves et al. [46] measured larger granulomas in BALB/c mice. In addition to high IFN-γ levels, we also saw significantly more eosinophils at week 10 post infection in the blood of BALB/c mice compared to C57BL/6 mice. This could imply that eosinophils in C57BL/6 mice were recruited to the liver tissue, because granulomas surrounding *S. mansoni* eggs are mainly composed of eosinophils [60, 61]. However, that eosinophil depletion did not change granuloma size in schistosome infected mice contradicts this idea [62]. Future studies could follow up on this observation using blood and whole spleen flow cytometry to distinguish the different immune cell populations in both *S. mansoni*-infected mouse hosts.

Of all measured cytokines, only IL-5 secretion had a significant impact on host-parasite interactions as assessed with GLM and ANOVA. IL-5 influences various cell types including B cells and eosinophils in a pleiotropic manner [63, 64]. This suggests that the four schistosome populations may differ in antigenicity, resulting in varying levels of induced inflammation affected by mouse host genetics. The fact that IL-5 is involved in fibrosis regulation, coupled with our analyses revealing a nearly significant impact of parasite population on fibrosis, supports this notion [65].

Parasite and host genotype impact different disease parameters

We found that parasite and host genotype impact different categories of disease parameters during infection and post sacrifice. Of four parasitological traits, parasite population strongly influenced the number of worms, liver egg burden and fecundity, whereas host influenced liver egg burden only. In contrast, host genotype impacted seven of 13 traits related to the immunological profile, with no discernible impact from the parasite population. In the immunopathology category (six traits), parasite genotype influenced three traits (liver weight, spleen weight and fibrosis), while host genotype also influenced three traits (spleen weight, weight gain, and fibrotic area). Hence, the severity of immunopathology observed is dependent on both parasite and host.

Limitations of this study

The influence of parasite genetics on immunopathological parameters measured in this study is probably conservative. Laboratory schistosome populations maintain surprisingly high levels of genetic and phenotypic variation (Jutzeler et al., unpublished observations) [18, 19, 66]. By infecting mice with genetically diverse schistosome larvae from four parasite populations, we captured an average phenotype for each population, so extreme phenotype traits were masked. We expect that use of genetically homogeneous parasite populations would result in much larger effects of parasite genotype. Future studies could focus on phenotype measures in mice infected with inbred schistosome lines generated by serial inbreeding over several generations. Such inbred schistosome lines are not currently available but could provide a valuable resource for investigating the role of parasite genetics in determining outcome of infection.

Similarly, we probably overestimated the role of host genetics by conducting these experiments using two inbred mouse strains known to show divergent immune responses to infection. Future work on host influences on schistosome immunopathology could use inbred mouse lines from the collaborative cross to determine the host genes involved [67].

Conclusions

This study highlights the significant influence of both schistosome parasite and mouse host genetics on immunopathological parameters. We found that (i) parasite population influenced liver and spleen weight and fibrotic area, (ii) both differences in total egg burden between parasite populations and intrinsic parasite

factors unrelated to egg burden contribute to immunopathology, and (iii) there were significant host-parasite interactions on IL-5 production. We anticipate that the impact of parasite genotype on immunopathology will be more pronounced when using inbred parasite populations; such inbred lines could also simplify genetic analysis of immunopathology traits.

Supplementary Information

The online version contains supplementary material available at https://doi.org/10.1186/s13071-024-06286-6.

Additional file 1: Table S1. Table showing detailed information, including weight change, of the mice that did not survive the entire infection period.

Additional file 2: Figure S1. Box plot showing the ratio of liver eggs to intestine eggs in schistosome-infected BALB/c (left) and C57BL/6 mice (right). Statistical comparison between parasite populations done for each host with Kruskal-Wallis (K-W) or ANOVA (BALB/c: Kruskal-Wallis; H = 4.26, df = 3, $P = 0.235$; C57BL/6: ANOVA; $F_{(3, 12)} = 1.34$, $P = 0.306$). Differences between hosts were not significant (Wilcox test; W = 97, $P = 0.109$).

Additional file 3: Figure S2. Intestine length of schistosome-infected BALB/c and C57BL/6 mice. Box plot showing intestine length in BALB/c (left) and C57BL/6 mice (right) infected with the four parasite populations or uninfected controls. Photos (right) show representative intestine samples from C57BL/6 mice infected with the four parasite populations and the control group for reference. Kruskal-Wallis to identify comparisons between parasite populations (BALB/c: H = 7.29, $P = 0.063$; C57BL/6: H = 6.38, $P = 0.094$) and Wilcoxon test to compare hosts, which were not significant.

Additional file 4: Figure S3. Neutrophil and reticulocyte levels and mean hematocrit (HCT) output. Longitudinal plots showing select CBC levels in BALB/c (top) and C57BL/6 mice (bottom) infected with the four parasite populations (solid lines) or uninfected control (dashed lines). **A** Neutrophil levels (Wilcoxon test to compare hosts: Baseline: W = 264, $P = 0.042$; Week 4: W = 275, $P = 0.034$). **B** Hematocrit (HCT) (Friedman; BALB/c: $\chi 2 = 16.4$, df = 3, $P < 0.001$; C57BL/6: $\chi 2 = 13.8$, df = 3, $P = 0.003$). Plot shows significant differences between hosts at baseline, and weeks 4, 6 and 8 (Wilcoxon test; Baseline: W = 101, $P = 0.032$; Week 4: W = 84, $P = 0.016$; Week 6: W = 77, $P = 0.016$; Week 8: W = 94.5, $P = 0.026$). **C** Reticulocyte production (Friedman; BALB/c: $\chi 2 = 10$, df = 3, $P = 0.019$; C57BL/6: $\chi 2 = 9.8$, df = 3, $P = 0.020$). #$P < 0.05$, ##$P < 0.01$, ###$P < 0.001$: values are significantly different between host strains.

Additional file 5: Figure S4: No differences in IL-2, IL-10 and IL-13 levels. **A** Despite a significant Kruskal-Wallis test in BALB/c mice (Kruskal-Wallis; BALB/c: H = 8.2, df = 3, $P = 0.042$; C57BL/6: H = 0.886, df = 3, $P = 0.829$), IL-2 secretion was not significantly different between parasite populations as analyzed by a Dunn post hoc test. **B** IL-10 (Kruskal-Wallis; BALB/c: H = 4.39, df = 3, $P = 0.223$; C57BL/6: H = 2.48, df = 3, $P = 0.479$) and **C** IL-13 (Kruskal-Wallis; BALB/c: H = 1.88, df = 3, $P = 0.597$; C57BL/6: H = 1.98, df = 3, $P = 0.576$) levels were not significantly different between parasite populations or mouse lines. K-W = Kruskal-Wallis.

Additional file 6: Figure S5: Correlation plots between total egg counts and liver/spleen weight. **A** Normalized liver weight is not significantly correlated in any of the parasite populations (Spearman's correlation coefficient; BRE: $rs = 0.47$, $P = 0.213$, EG: $rs = 0.095$, $P = 0.840$, LE: $rs = 0.43$, $P = 0.299$, OR: $rs = 0.63$, $P = 0.076$). **B** Normalized spleen weight does not significantly correlate with total egg burden in the four parasite populations examined (Spearman's correlation coefficient; BRE: $rs = 0.43$, $P = 0.25$, EG: $rs = 0.19$, $P = 0.665$, LE: $rs = -0.024$, $P = 0.977$, OR: $rs = 0.33$, $P = 0.385$).

Additional file 7: Table S1. Zenodo repository information for histology images.

Acknowledgements
We thank the animal care staff of the Southwest National Primate Research Center (SNPRC) for providing rodent care, training and equipment to perform this study; Renee Escalona, Colin Chuba and Jesse Martinez from the Hixon Pathology core lab (Texas Biomedical Research Institute) for performing all the histopathology preparations and staining of mouse livers, Dr. Vinay Shivanna for providing access to the HALO software for analyzing the histopathology slides and Dr. Vida Hodara from the Biology core lab for processing the cytokine samples. Finally, we thank Dr. P'ng Loke, Chief of the Type 2 Immunity Section at the NIAID, and Dr. Reagan Meredith (Texas Biomedical Research Institute) for their input and recommendations regarding study design and statistical analysis respectively. We acknowledge the use of BioRender for creating the graphical abstract and Figure 1 in this manuscript.

Author contributions
KSJ and TJCA designed and planned the experiments. WL and FDC provided training and assisted with methodology. KSJ performed all the experiments (mouse infections, measurement of all the phenotypes in hosts and cytokine assay) and all the data analyses including liver histopathology. KSJ and TJCA drafted the manuscript. All authors read and approved the final manuscript.

Funding
This research was supported by a Graduate Research in Immunology Program training grant NIH T32 AI138944 (KSJ), and NIH R01 AI133749, R01 AI166049 (TJCA), and was conducted in facilities constructed with support from Research Facilities Improvement Program grant C06 RR013556 from the National Center for Research Resources. SNPRC research at Texas Biomedical Research Institute is supported by grant P51 OD011133 from the Office of Research Infrastructure Programs, NIH.

Availability of data and materials
The datasets supporting the conclusions of this article and all codes used for data analysis and generation of Figs. (2–6, S1-S5) are available at https://github.com/kathrinsjutzeler/sm_immunopathology/ and https://doi.org/https://doi.org/10.5281/zenodo.10465594. All histology images used in this manuscript were uploaded to Zenodo. Additional file 7 : Table S2 contains the description and repository information for each data set.

Declarations

Competing interests
The authors declare that they have no competing interests.

Received: 12 January 2024 Accepted: 18 April 2024
Published online: 07 May 2024

References

1. Aiewsakun P, Nilplub P, Wongtrakoongate P, Hongeng S, Thitithanyanont A. SARS-CoV-2 genetic variations associated with COVID-19 pathogenicity. Microb Genomics. 2021;7:000734. https://doi.org/10.1099/mgen.0.000734.
2. Mlcochova P, Kemp S, Dhar MS, Papa G, Meng B, Ferreira IATM, et al. SARS-CoV-2 B.1.617.2 Delta variant replication and immune evasion. Nature. 2021;599:114–9. https://www.nature.com/articles/s41586-021-03944-y.
3. Schulze H, Bayer W. Changes in symptoms experienced by SARS-CoV-2-infected individuals – from the first wave to the omicron variant. Front Virol. 2022;2:880707.
4. Mueller M, Tainter CR. *Escherichia coli* Infection. StatPearls. Treasure Island (FL): StatPearls Publishing; 2023 [cited 2023 Jun 6]. http://www.ncbi.nlm.nih.gov/books/NBK564298/
5. Kaper JB, Nataro JP, Mobley HLT. Pathogenic *Escherichia coli*. Nat Rev Microbiol. 2004;2:123–40.
6. Grace CA, Sousa-Carvalho KS, Sousa-Lima MI, Costa-Silva V, Reis-Cunha JL, Brune MJ, et al. Parasite genotype is a major predictor of mortality from visceral leishmaniasis. MBio. 2022;1:e02068-e2122.

7. Hotez PJ, Alvarado M, Basáñez M-G, Bolliger I, Bourne R, Boussinesq M, et al. The global burden of disease study 2010: interpretation and implications for the neglected tropical diseases. PLoS Negl Trop Dis. 2014;8:e2865.
8. World Health Organization. Soil-Transmitted Helminth Infections Fact Sheet [Internet]. Available from: https://www.who.int/news-room/fact-sheets/detail/soil-transmitted-helminth-infections.
9. Piecyk A, Roth O, Kalbe M. Specificity of resistance and geographic patterns of virulence in a vertebrate host-parasite system. BMC Evol Biol. 2019;19:80.
10. Nuaima RH, Heuer H. Genetic Variation among *Heterodera schachtii* populations coincided with differences in invasion and propagation in roots of a set of cruciferous plants. Int J Mol Sci. 2023;24:6848.
11. Wakelin D. Immunogenetic and evolutionary influences on the host-parasite relationship. Dev Comp Immunol. 1992;16:345–53.
12. Goyal PK, Wakelin D. Influence of variation in host strain and parasite isolate on inflammatory and antibody responses to *Trichinella spiralis* in mice. Parasitology. 1993;106:371–8.
13. LoVerde PT. Schistosomiasis. In: Toledo R, Fried B, editors. Digenetic Trematodes. Cham: Springer International Publishing; 2019. p. 45–70. Available from: https://doi.org/10.1007/978-3-030-18616-6_3.
14. William S, Day TA, Botros S, Tao LF, Bennett JL, Farghally A, et al. Resistance to praziquantel: direct evidence from *Schistosoma mansoni* isolated from Egyptian villagers. Am J Trop Med Hyg. 1999;60:932–5.
15. Melman SD, Steinauer ML, Cunningham C, Kubatko LS, Mwangi IN, Wynn NB, et al. Reduced susceptibility to praziquantel among naturally occurring Kenyan isolates of *Schistosoma mansoni*. PLoS Negl Trop Dis. 2009;3:e504.
16. Couto FFB, Coelho PMZ, Araújo N, Kusel JR, Katz N, Jannotti-Passos LK, et al. *Schistosoma mansoni*: a method for inducing resistance to praziquantel using infected *Biomphalaria glabrata* snails. Mem Inst Oswaldo Cruz. 2011;106:153–7.
17. Anderson TJC, LoVerde PT, Le Clec'h W, Chevalier FD. Genetic crosses and linkage mapping in schistosome parasites. Trends Parasitol. 2018;34:982–96.
18. Le Clec'h W, Diaz R, Chevalier FD, McDew-White M, Anderson TJC. Striking differences in virulence, transmission and sporocyst growth dynamics between two schistosome populations. Parasit Vectors. 2019;12:485.
19. Le Clec'h W, Chevalier FD, Jutzeler K, Anderson TJC. No evidence for schistosome parasite fitness trade-offs in the intermediate and definitive host. Parasit Vectors. 2023;16:132.
20. Anderson LA, Cheever AW. Comparison of geographical strains of *Schistosoma mansoni* in the mouse. Bull World Health Organ. 1972;46:233–42.
21. Soliman GN, Assal FM, Mansour NS, Garo K. Comparison of two egyptian strains of *Schistosoma mansoni* in hamsters. Z Für Parasitenkd Parasitol Res. 1986;72:353–63.
22. Euzébio AA, Zuim NRB, Linhares AX, Magalhães LA, Zanotti-Magalhães EM. Experimental evaluation of the pathogenicity of different strains of *Schistosoma mansoni*. Interdiscip Perspect Infect Dis. 2012;2012:1–7.
23. Nino Incani R, Morales G, Cesari IM. Parasite and vertebrate host genetic heterogeneity determine the outcome of infection by *Schistosoma Mansoni*. Parasitol Res. 2001;87:131–7.
24. Cioli D, Pica-Mattoccia L, Moroni R. *Schistosoma mansoni*: hycanthone/oxamniquine resistance is controlled by a single autosomal recessive gene. Exp Parasitol. 1992;75:425–32.
25. Valentim CLL, Cioli D, Chevalier FD, Cao X, Taylor AB, Holloway SP, et al. Genetic and molecular basis of drug resistance and species-specific drug action in Schistosome parasites. Science. 2013;342:1385–9.
26. Mills CD, Kincaid K, Alt JM, Heilman MJ, Hill AM. M-1/M-2 Macrophages and the Th1/Th2 Paradigm. J Immunol. 2000;164:6166–73.
27. Fukushima A, Yamaguchi T, Ishida W, Fukata K, Taniguchi T, Liu F-T, et al. Genetic background determines susceptibility to experimental immune-mediated blepharoconjunctivitis: comparison of Balb/c and C57BL/6 mice. Exp Eye Res. 2006;82:210–8.
28. Sellers RS, Clifford CB, Treuting PM, Brayton C. Immunological variation between inbred laboratory mouse strains: points to consider in phenotyping genetically immunomodified mice. Vet Pathol. 2012;49:32–43.
29. Yagi J, Arimura Y, Takatori H, Nakajima H, Iwamoto I, Uchiyama T. Genetic background influences Th cell differentiation by controlling the capacity for IL-2-induced IL-4 production by naive CD4+ T cells. Int Immunol. 2006;18:1681–90.
30. McCarthy D, Reinertson JW, Thompson PE. A Convenient Device for Exposing Mice to *Schistosoma mansoni* by Tail Immersion. J Parasitol. 1954;40:704.
31. Molehin AJ. Current understanding of immunity against schistosomiasis: impact on vaccine and drug development. Res Rep Trop Med. 2020;11:119–28.
32. Zheng B, Zhang J, Chen H, Nie H, Miller H, Gong Q, et al. T Lymphocyte-mediated liver immunopathology of schistosomiasis. Front Immunol. 2020;11:61.
33. DeWitt WB, Duvall RH. An improved perfusion technique for recovering adult schistosomes from laboratory animals. Am J Trop Med Hyg. 1967;16:483–6.
34. Schindelin J, Rueden CT, Hiner MC, Eliceiri KW. The ImageJ ecosystem: an open platform for biomedical image analysis. Mol Reprod Dev. 2015;82:518–29.
35. Van De Vlekkert D, Machado E, d'Azzo A. Analysis of generalized fibrosis in mouse tissue sections with Masson's trichrome staining. Bio-Protoc. 2020;10:e3629.
36. R Core Team. R: A language and environment for statistical computing. R Foundation for Statistical Computing, Vienna, Austria.; 2022. Available from URL https://www.R-project.org/.
37. Kassambara A. rstatix: Pipe-Friendly Framework for Basic Statistical Tests [Internet]. 2023. Available from: https://CRAN.R-project.org/package=rstatix>
38. Benjamini Y, Hochberg Y. Controlling the false discovery rate: a practical and powerful approach to multiple testing. J R Stat Soc Ser B Methodol. 1995;57:289–300.
39. Neath AA, Cavanaugh JE. The Bayesian information criterion: background, derivation, and applications. WIREs Comput Stat. 2012;4:199–203.
40. Ben-Shachar M, Lüdecke D, Makowski D. Effectsize: estimation of effect size indices and standardized parameters. J Open Source Softw. 2020;5:2815.
41. Hackey JR, Stirewalt MA. Penetration of host skin by cercariae of *Schistosoma mansoni*. I. Observed entry into skin of mouse, hamster, rat, monkey and man. J Parasitol. 1956;42:565–80.
42. Membe Femoe U, Boukeng Jatsa H, Greigert V, Brunet J, Cannet C, Kenfack MC, et al. Pathological and immunological evaluation of different regimens of praziquantel treatment in a mouse model of *Schistosoma mansoni* infection. PLoS Negl Trop Dis. 2022;16:e0010382.
43. Coutinho EM, Silva FL, Barros AF, Araújo RE, Oliveira SA, Luna CF, et al. Repeated infections with *Schistosoma mansoni* and liver fibrosis in undernourished mice. Acta Trop. 2007;101:15–24.
44. Maciel PS, Gonçalves R, Antonelli LRV, Fonseca CT. *Schistosoma mansoni* infection is impacted by malnutrition. Front Microbiol. 2021;12:635843.
45. Schwartz C, Fallon PG. *Schistosoma* "Eggs-Iting" the host: granuloma formation and egg excretion. Front Immunol. 2018;9:2492.
46. Alves CC, Araujo N, Cassali GD, Fonseca CT. Parasitological, pathological, and immunological parameters associated with *Schistosoma mansoni* infection and reinfection in BALB/c AND C57BL/6 Mice. J Parasitol. 2016;102:336.
47. Cheever AW, Hallack TA, Minker RG, Duvall RH, Malley JD, Malley KG. Variation of hepatic fibrosis and granuloma size among mouse strains infected with *Schistosoma mansoni*. Am J Trop Med Hyg. 1987;37:85–97.
48. Anthony RM, Rutitzky LI, Urban JF, Stadecker MJ, Gause WC. Protective immune mechanisms in helminth infection. Nat Rev Immunol. 2007;7:975–87.
49. Skelly PJ, Da'dara AA, Li X-H, Castro-Borges W, Wilson RA Schistosome Feeding and Regurgitation. PLoS Pathog. 2014;10:e1004246. https://doi.org/10.1371/journal.ppat.1004246.
50. Bärenbold O, Garba A, Colley DG, Fleming FM, Assaré RK, Tukahebwa EM, et al. Estimating true prevalence of *Schistosoma mansoni* from population summary measures based on the Kato-Katz diagnostic technique. PLoS Negl Trop Dis. 2021;15:e0009310.
51. Spencer SA, Penney JMSJ, Russell HJ, Howe AP, Linder C, Rakotomampianina ALD, et al. High burden of *Schistosoma mansoni* infection in school-aged children in Marolambo District. Madagascar Parasit Vectors. 2017;10:307.
52. Abudho BO, Guyah B, Ondigo BN, Ndombi EM, Ireri E, Carter JM, et al. Evaluation of morbidity in *Schistosoma mansoni*-positive primary and secondary school children after four years of mass drug administration of praziquantel in western Kenya. Infect Dis Poverty. 2020;9:67.

53. Le Clec'h W, Chevalier FD, McDew-White M, Menon V, Arya G-A, Anderson TJC. Genetic architecture of transmission stage production and virulence in schistosome parasites. Virulence. 2021;12:1508–26.
54. Bin Dajem SM, Mostafa OMS, El-Said FG. Susceptibility of two strains of mice to the infection with *Schistosoma mansoni*: Parasitological and biochemical studies. Parasitol Res. 2008;103:1059–63.
55. Simon MM, Greenaway S, White JK, Fuchs H, Gailus-Durner V, Wells S, et al. A comparative phenotypic and genomic analysis of C57BL/6J and C57BL/6N mouse strains. Genome Biol. 2013;14:R82.
56. Czaja MJ, Weiner FR, Takahashi S, Giambrone MA, van der Meide PH, Schellekens H, et al. Gamma-interferon treatment inhibits collagen deposition in murine schistosomiasis. Hepatol Baltim Md. 1989;10:795–800.
57. Koo GC, Gan Y-H. The innate interferon gamma response of BALB/c and C57BL/6 mice to in vitro *Burkholderia pseudomallei* infection. BMC Immunol. 2006;7:19.
58. La Flamme AC, Patton EA, Pearce EJ. Role of gamma interferon in the pathogenesis of severe schistosomiasis in interleukin-4-deficient mice. Infect Immun. 2001;69:7445–52.
59. Hoffmann KF, Cheever AW, Wynn TA. IL-10 and the dangers of immune polarization: excessive type 1 and type 2 cytokine responses induce distinct forms of lethal immunopathology in murine schistosomiasis. J Immunol. 2000;164:6406–16.
60. Llanwarne F, Helmby H. Granuloma formation and tissue pathology in *Schistosoma japonicum* versus *Schistosoma mansoni* infections. Parasite Immunol. 2021;43:1. https://doi.org/10.1111/pim.12778.
61. Domingo EO, Warren KS. Granuloma Formation around *Schistosoma Mansoni*, *S. Haematobium*, and *S. Japonicum* eggs: size and rate of development, cellular composition, cross-sensitivity, and rate of egg destruction. Am J Trop Med Hyg. 1970;19:292–304.
62. Swartz JM, Dyer KD, Cheever AW, Ramalingam T, Pesnicak L, Domachowske JB, et al. *Schistosoma mansoni* infection in eosinophil lineage-ablated mice. Blood. 2006;108:2420–7.
63. Takatsu K. Interleukin-5 and IL-5 receptor in health and diseases. Proc Jpn Acad Ser B. 2011;87:463–85.
64. Rosa Brunet L, Sabin EA, Cheever AW, Kopf MA, Pearce EJ. Interleukin 5 (IL-5) Is Not Required for Expression of a Th2 Response or Host Resistance Mechanisms during Murine Schistosomiasis Mansoni but Does Play a Role in Development of IL-4-Producing Non-T. Non-B Cells Infect Immun. 1999;67:3014–8.
65. Reiman RM, Thompson RW, Feng CG, Hari D, Knight R, Cheever AW, et al. Interleukin-5 (IL-5) augments the progression of liver fibrosis by regulating IL-13 Activity. Infect Immun. 2006;74:1471–9.
66. Le Clec'h W, Chevalier FD, Mattos ACA, Strickland A, Diaz R, McDew-White M, et al. Genetic analysis of praziquantel response in schistosome parasites implicates a transient receptor potential channel. Sci Transl Med. 2021;13:9114.
67. Threadgill DW, Miller DR, Churchill GA, de Villena FP-M. The collaborative cross: a recombinant inbred mouse population for the systems genetic era. ILAR J. 2011;52:24–31.

Publisher's Note